Report No. FAA-RD-75-155

IGNITION AND PROPAGATION RATES FOR FLAMES IN A FUEL MIST

C. E. Polymeropoulos

OCTOBER 1975

INTERIM REPORT

Prepared for

U. S. DEPARTMENT OF TRANSPORTATION
FEDERAL AVIATION ADMINISTRATION
Systems Research & Development Service
Washington, D. C. 20590

METRIC CONVERSION FACTORS

Approximate Conversions to Metric Measures

Symbol	When You Know	Multiply by	To Find	Symbol
	LENGTH			
in	inches	*2.5	centimeters	cm
ft	feet	30	centimeters	cm
yd	yards	0.9	meters	m
mi	miles	1.6	kilometers	km
	AREA			
in^2	square inches	6.5	square centimeters	cm^2
ft^2	square feet	0.09	square meters	m^2
yd^2	square yards	0.8	square meters	m^2
mi^2	square miles	2.6	square kilometers	km^2
	acres	0.4	hectares	ha
	MASS (weight)			
oz	ounces	28	grams	g
lb	pounds	0.45	kilograms	kg
	short tons (2000 lb)	0.9	tonnes	t
	VOLUME			
tsp	teaspoons	5	milliliters	ml
Tbsp	tablespoons	15	milliliters	ml
fl oz	fluid ounces	30	milliliters	ml
c	cups	0.24	liters	l
pt	pints	0.47	liters	l
qt	quarts	0.95	liters	l
gal	gallons	3.8	liters	l
ft^3	cubic feet	0.03	cubic meters	m^3
yd^3	cubic yards	0.76	cubic meters	m^3
	TEMPERATURE (exact)			
°F	Fahrenheit temperature	5/9 (after subtracting 32)	Celsius temperature	°C

*1 in = 2.54 (exactly). For other exact conversions and more detailed tables, see NBS Misc. Publ. 286, Units of Weights and Measures, Price $2.25, SD Catalog No. C13.10:286.

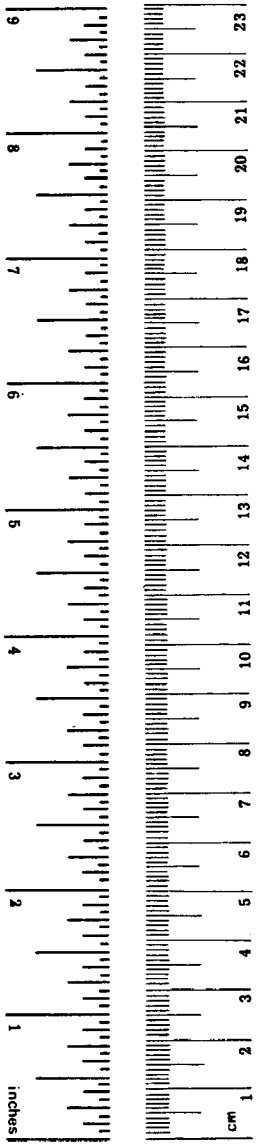

Approximate Conversions from Metric Measures

Symbol	When You Know	Multiply by	To Find	Symbol
	LENGTH			
mm	millimeters	0.04	inches	in
cm	centimeters	0.4	inches	in
m	meters	3.3	feet	ft
m	meters	1.1	yards	yd
km	kilometers	0.6	miles	mi
	AREA			
cm^2	square centimeters	0.16	square inches	in^2
m^2	square meters	1.2	square yards	yd^2
km^2	square kilometers	0.4	square miles	mi^2
ha	hectares (10,000 m^2)	2.5	acres	
	MASS (weight)			
g	grams	0.035	ounces	oz
kg	kilograms	2.2	pounds	lb
t	tonnes (1000 kg)	1.1	short tons	
	VOLUME			
ml	milliliters	0.03	fluid ounces	fl oz
l	liters	2.1	pints	pt
l	liters	1.06	quarts	qt
l	liters	0.26	gallons	gal
m^3	cubic meters	35	cubic feet	ft^3
m^3	cubic meters	1.3	cubic yards	yd^3
	TEMPERATURE (exact)			
°C	Celsius temperature	9/5 (then add 32)	Fahrenheit temperature	°F

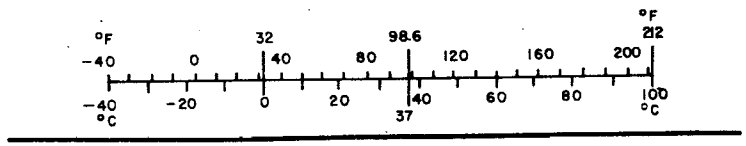

TECHNICAL REPORT STANDARD TITLE PAGE

1. Report No.	2. Government Accession No.	3. Recipient's Catalog No.
FAA-RD-75-155		

4. Title and Subtitle	5. Report Date
IGNITION AND PROPAGATION RATES FOR FLAMES IN A FUEL MIST	April 1975
	6. Performing Organization Code

7. Author(s)	8. Performing Organization Report No.
C. E. Polymeropoulos	FAA-NA-75-153

9. Performing Organization Name and Address	10. Work Unit No.
Department of Mechanical, Industrial and Aerospace Engineering Rutgers, The State University of New Jersey New Brunswick, New Jersey 08903	11. Contract or Grant No. DOT FA 72 NA-746
	13. Type of Report and Period Covered Interim Report July 1972 - January 1975
12. Sponsoring Agency Name and Address U.S. Department of Transportation Federal Aviation Administration Systems Research and Development Service Washington, D.C. 20590	14. Sponsoring Agency Code

15. Supplementary Notes

The contract was administered by the National Aviation Facilities Experimental Center, Atlantic City, New Jersey 08405.

16. Abstract

A mathematical model was developed, which is capable of predicting the burning velocity in polydisperse air-fuel sprays given the initial conditions of the liquid and gas phases. The analytical predictions were tested against previous experimental data, and the agreement was satisfactory.

The burning velocity in polydisperse kerosene-air sprays was measured at constant air-fuel ratio, and for various degrees of atomization of the spray in order to further check the predictions of the mathematical model. The results were also in good agreement with the analytical predictions.

17. Key Words	18. Distribution Statement
Fuels Droplets Sprays Burning Velocity	Document is available to the public through the National Technical Information Service, Springfield, Virginia 22151

19. Security Classif. (of this report)	20. Security Classif. (of this page)	21. No. of Pages	22. Price
Unclassified	Unclassified	61	

Form DOT F 1700.7 (8-69)

PREFACE

This report was prepared by the Mechanical, Industrial and Aerospace Engineering Department at Rutgers, The State University of New Jersey, for the Federal Aviation Administration. From July, 1972, to July, 1973, the work was carried out under the management of Mr. R. A. Russell, and from August, 1973, to January, 1975, under the management of Mr. S. Zinn. The project managers are from the Propulsion-Fire Protection Branch, Aircraft and Airport Safety Division, National Aviation Facilities Experimental Center, Atlantic City, New Jersey.

TABLE OF CONTENTS

LIST OF ILLUSTRATIONS

LIST OF TABLES

LIST OF ABBREVIATIONS AND SYMBOLS

B	$B_o T^{\frac{1}{2}}$
B_o	frequency constant
c_p	specific heat of the gas mixture
C_D	drag coefficient
$\overline{d}$	Sauter mean diameter
D	binary diffusion coefficient
E	activation energy
f_i	δ_{fi} before droplet ignition
	α_i, $i = 0, P$, after droplet ignition
h_j	heat transfer coefficient
H	enthalpy
H^o	standard enthalpy of formation
$\dot{H}_s$	spray enthalpy flux
k	thermal conductivity
L	latent heat of vaporization for the fuel
$\dot{m}$	total evaporation rate of the spray
M	molecular weight of the gas mixture
$\dot{M}$	mixture mass flux
n	number of droplet size groups
n_i	mole fraction of species i
N_j	number density of droplet group j
p	pressure
Q	heat of reaction for the fuel
r	radial distance from tube axis
R	tube radius
$\overline{R}$	universal gas constant
R_j	radius of droplet group j
Re_j	Reynolds number of droplet group j
S	defined in equation 29
S_u	experimentally determined burning velocity
T	absolute temperature
T_I	ignition temperature
T_r	reference temperature
t	time
u'	rms velocity fluctuation
u_j	speed of droplet group j
v	gas speed
V_s	spray volume
w_i	mass rate of production for species i per unit volume
x	downstream distance
Y_i	mass fraction of species i
Z	$z/(\exp(z)-1)$
z	defined in equation 6

Greek Symbols

α_i	stoichiometric mass coefficient for species i
$\Delta\ell$	distance along the flame front
Δr	distance along the tube axis
ε	eddy diffusivity
λ	characteristic turbulent length scale
μ	viscosity of the gas
ν	kinematic viscosity of the gas
ρ	density
ϕ	fuel-air ratio / stoichiometric fuel-air ratio

Subscripts

B	boiling point
F	fuel species
g	gaseous phase
I	ignition condition
i	F, O, P, N refers to the species present
j	droplet size group j
L	downstream boundary
ℓ	liquid
m	denotes grid point
N	neutrals
o	upstream boundary
O	oxidizer
P	products
s	refers to the spray
t	refers to turbulent transport properties

INTRODUCTION

PURPOSE.

The purpose of this research effort was to develop a mathematical model for predicting ignition and propagation rates for flames in a fuel mist.

This report describes the model that was developed, and includes comparisons of the theoretical predictions with experimental data on tetralin-air sprays obtained by previous investigators.

In addition, this report describes experiments that were carried out for measuring burning velocities in kerosene-air sprays, and includes comparisons of experimental data with predicted values from the theoretical model.

BACKGROUND.

The work described in this report is related to the burning of fuel in mist or fine spray form during an aircraft crash, and is aimed at identifying pertinent parameters which control the propagation of a flame in a combustible liquid fuel mist. Since the principal interest is in aircraft crash fire safety, the analysis and experimentation are related to burning under atmospheric conditions and to kerosene based fuels. In addition, experimental data from previous investigators (1-3) who employed tetralin-air sprays are used for comparisons with the theoretical predictions of the present work.

The report consists of two principal parts: the first part describes the mathematical model and the results of the numerical computations that were carried out, while the second part contains a description of experimental work on the effect of droplet size on the burning velocity of polydisperse kerosene-air sprays. Instructions for the use of the computer program for calculating burning velocities, and a listing of the program in the Fortran IV language are found in Appendices A and B, respectively.

The work presented in this report has in part appeared in references (4,5).

MATHEMATICAL MODEL

SPRAY MODEL.

GENERAL DESCRIPTION AND ASSUMPTIONS. Propagation of flame in a dilute liquid fuel spray has been studied by several investigators because of its importance to flame stabilization and spray burning. Burgoyne and Cohen (1), Burgoyne (2), and Mizutani and Ogasawara (3) have measured one-dimensional laminar flame propagation velocities in monodisperse sprays. Their results showed that with very small droplets and very dilute sprays the propagation

mechanism is that of a premixed flame, while with large droplets the mechamism is through a relay transfer of the flame from droplet to droplet. Williams (6), using separate analyses for very small and for large droplets, has obtained satisfactory agreement with the results of Burgoyne et al (1), within the accuracy of the assumptions and the constant property values used in the calculations. Measurements of burning velocities in one-dimensional polydisperse sprays have also been reported (7-10) as well as calculated results for pure vaporization (11), and burning (12) of such sprays. In a recent study Mizutani (13) presented calculations for the burning velocity in turbulent polydisperse sprays neglecting preignition vaporization. There is also a considerable body of work related to liquid fuel rocket combustors which was disucssed by Sutton et al (14). The authors of the last reference also describe their three-dimensional analysis and modeling for the burning of a liquid fuel spray. However, as with most other works related to liquid fuel rockets, their analysis does not address itself directly to the flame propagation problem.

The burning of a liquid fuel spray is a process involving complex transient interactions between the droplets and the surrounding gas phase. The gas flow is usually turbulent, and the spray is distributed among different droplet sizes, which move at different velocities and are randomly distributed in space. To simplify the fluid dynamical calculation, the calculations of spray burning velocities were carried out using a one-dimensional flow model. A dilute spray initially consisting of a stream of air and liquid fuel droplets is assumed to pass through a plane heat source located perpendicular to the flow direction as shown in Figure 1. The heat source both increases the gas temperature to a level that is sufficient to ignite the fuel so that combustion is completed within the domain of the numerical computation, and fixes the position of the flame during the calculations. Under these conditions steady state combustion always takes place downstream from the heat source, provided that the velocity of the gas stream is higher than the burning velocity in the spray. The lowest gas velocity for which the spray can exist in steady state is the burning velocity for normal flame propagation. It also identifies the upstream conditions for "flash-back" from a plane heat source. It should be noted that the results are expected to apply only to cases where the droplet trajectories follow the streamlines of the gas. The mathematical formulation follows the analysis of Williams and Sutton et al (14), and employs the following general assumptions:

1. The gas flow is one-dimensional, steady, at constant pressure, and obeys the ideal gas equation. Thermal radiation effects are neglected.

2. The gaseous mixture in each section is homogeneous. This implies that there is an instantaneous mixing of the species, and that the presence of the liquid phase affects the gas flow only through source and sink terms for species produced or consumed around the droplets.

3. The mixture flow is adiabatic except at the location of the plane heat source.

4. The spray is dilute, and the distribution of droplet sizes is described in terms of a finite number of size groups. There is no interaction between droplets during evaporation or combustion.

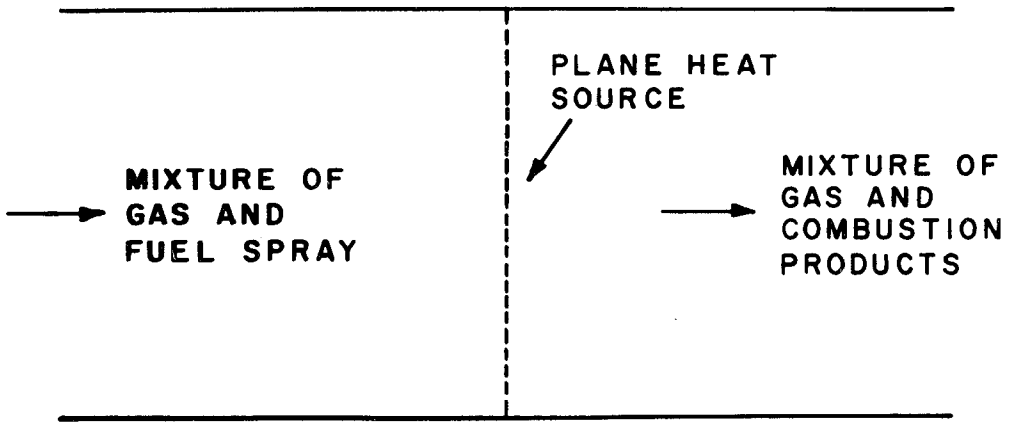

FIGURE 1. SCHEMATIC DIAGRAM OF FUEL SPRAY AND PLANE HEAT SOURCE

5. For the small relative velocities considered here, the droplets do not deform or shatter but are influenced by aerodynamic drag forces.

6. The droplet evaporation rate follows stagnant film relationships for pre- and post-ignition vaporization, corrected for forced convection.

7. Droplet ignition occurs when the liquid temperature reaches the level necessary for the formation of a stoichiometric fuel-air mixture at the liquid surface. According to reference 15 for hydrocarbon fuels this occurs when the liquid temperature, T_ℓ, is given by:

$$T_\ell = 0.74\ T_B - 70\ [^oC] \qquad (1)$$

where T_B is the liquid boiling point. Reference 15 suggests that for sufficiently high ambient air temperatures equation (1) results in a reasonable approximation of the ignition delay period. Before ignition the droplets act as sources of fuel vapor for the ambient gas. After ignition occurs, the consumption of fuel and oxidizer and the generation of products of combustion around the droplets follow the stoichiometry of fuel combustion.

Previous calculations (4) employed a prescribed gas temperature as the ignition criterion, regardless of the previous history of the droplets. The use of a prescribed ignition temperature simplifies the description of the transient droplet behavior through the ignition point, but underestimates the ignition delay for the droplets. Results were, therefore, presented (4) for various ignition temperatures, which is equivalent to changing the ignition delay time. The use of equation (1) as the ignition criterion implies a dependence on droplet size, since the time for reaching T_ℓ depends on the droplet diameter. However, T_ℓ does not depend on the ambient oxygen concentration. This, however, does not limit the usefulness of the results with respect to dilute sprays involved in aircraft crashes.

8. The equations describing the gas flow are written in terms of four species: fuel, oxidizer, products, and neutrals. They include the effects of conduction heat transfer and diffusion of species and are coupled to the liquid phase equations through appropriate source, or sink, terms for energy and mass transport. Chemical reactions for the fuel vapor, which is added to the homogeneous gas phase during the droplet pre-ignition vaporization period, are described in terms of one second order rate controlling step. The necessary chemical kinetic parameters are adjusted to give agreement with available experimental data.

9. Physical properties are computed for each downstream position and depend on the local gas phase temperature and concentration.

10. Boundary conditions include (a) the upstream temperature, velocity, and combustion of the spray, and (b) the downstream absence of any fuel as liquid or vapor. It is also necessary to specify the intensity and position of the plane heat source.

11. Turbulent sprays are described in terms of an eddy diffusivity model as in reference 13. Although this model does not represent the physical processes occurring in wrinkled flames, when the scale of turbulence is larger than the flame front thickness, it at least gives a reasonable qualitative variation of the effects of turbulence on the burning velocity. It is also assumed that there is no effect of the flame on the scale and intensity of turbulence.

LIQUID PHASE EQUATIONS.

a. Droplet flux balance:

$$N_j u_j = N_{jo} u_{jo} \tag{2}$$

where N_j is the number density of droplet group j which is moving with a velocity u_j, j = 1, ...n. n is the number of droplet groups at the upstream boundary which is denoted by the subscript $_o$.

b. Droplet momentum balance:

$$u_j \frac{du_j}{dx} = \frac{3}{8} \frac{\rho_g}{\rho_\ell} \frac{(v-u_j)}{R_j} |v-u_j| \, C_{Dj} \tag{3}$$

The drag coefficient is $C_{Dj} = 27/Re_j^{0.8}$, (Reference 16). v is the gas speed, R_j is the radius of droplet group j, $Re_j = 2R_j|v-u_j|/\nu$ is the Reynolds number, and ρ_g and ρ_ℓ are the gas liquid phase densities, respectively. ρ_ℓ is assumed to be constant.

c. Droplet energy balance:

$$Zh_j (T-T_j) = -\frac{dR_j}{dt} \rho_\ell L + C_{p\ell} \rho_\ell R_j \frac{1}{3} \frac{dT_j}{dt} \tag{4}$$

The heat transfer coefficient h_j is given by the relationship of Ranz et al (17):

$$\frac{2R_j h_j}{k} = 2 + 0.6 Re_j^{0.5} \tag{5}$$

where k is the thermal conductivity of the gas. T_j is the droplet temperature, which is assumed uniform within the drop. L is the heat of vaporization and $c_{p\ell}$ is the heat capacity of the fuel, which is assumed to be constant. Z is a correction factor for using equation (5) with droplets where vaporization is appreciable. It is the ratio of the droplet heat transfer coefficient with vaporization to that with negligible vaporization. It is given by (reference 16)

$$Z = \frac{z}{\exp(z)-1} \tag{6}$$

where

$$z = -2R_j \frac{dR_j}{dt} \frac{c_{pf}\rho_\ell}{k \, Nu_j} \tag{7}$$

d. Droplet evaporation rate:

The following equation was used for the rate of radius change of burning droplets (8):

$$\frac{dR_j}{dt} = -\frac{k}{R_j c_p} \ln \left[1 + \frac{c_p(T-T_j)}{L} - \frac{QY_0}{\alpha_0 L} \right] \tag{8}$$

where Q is the heat of reaction for the fuel, Y_0 is the local oxidizer mass fraction, α_0 is the stoichiometric coefficient for the oxidizer, and c_p is the local value of specific heat for the gas. For quasi-steady state evaporation without burning, equation (8) was used without the term $(QY_0/\alpha_0 L)$, provided the droplet temperature was near the liquid fuel boiling point. The initial transient preheat and vaporization period was described by the following relationship (18):

$$\frac{dR_j}{dt} = -\frac{k}{c_p \rho_\ell} \frac{(Nu_j Z)}{2R_j} \left[\frac{Y_{Fj} - Y_F}{1 - Y_{Fj}} \right] \tag{9}$$

where it is assumed that the heat and mass transfer processes around a droplet are similar. The fuel mass fraction at the droplet surface, Y_{Fj}, is given by the Clapeyron equation:

$$Y_{Fj} = \frac{M_F}{M} \exp \left[\frac{LM}{R} \left(\frac{1}{T_B} - \frac{1}{T_j} \right) \right] \tag{10}$$

e. Spray evaporation rate:

$$\dot{m} = -\sum_j N_j \rho_\ell 4\pi R_j^2 \frac{dR_j}{dt} \tag{11}$$

where $\dot{m}$ is the spray evaporation rate.

f. Spray enthalpy flux:

$$\dot{H}_s = \sum_j N_j u_j \rho_\ell 4\pi R_j^2 \frac{dR_j}{dt} \left[\int_{T_r}^{T_j} c_{p\ell} dT + H^o_{F\ell} \right] \tag{12}$$

where $\dot{H}_s$ is the spray enthalpy flux, and H^o_F is the standard enthalpy of formation for the liquid fuel taken at temperature T_r.

Equations (11) and (12) together with the expression for spray volume:

$$V_s = \sum_j N_j \frac{4\pi}{3} R_j^3 \tag{13}$$

provide the necessary coupling terms between the liquid and the gas phase.

GAS PHASE EQUATIONS.

For constant pressure and low speed flow of a dilute spray the momentum equation for the gas flow can be neglected. The remaining equations for the gas are as follows:

a. Global continuity:

$$\rho_g u + \sum_j N_j u_j \rho_\ell \frac{4\pi}{3} R_j^3 = \dot{M} \tag{14}$$

where $\dot{M} = \rho_{go} u_o + \sum_j N_{jo} u_{jo} \rho_\ell$ is the mass flux for the mixture.

b. Species conservation:

$$\frac{d}{dx}(\rho_g v Y_i) - \frac{d}{dx}(\rho_g D_i \frac{dY_i}{dx}) = w_i + \dot{m} f_i \tag{15}$$

$$i = F, O, P, N$$

where Y_i is the mass fraction for species i, and D_i is the binary diffusion coefficient for the ith species. The term $\dot{m} f_i$ in equation (15) refers to the volumetric rate of species produced or consumed within the boundary layer of the droplets in the spray. Before ignition $f_i = \delta_{Fi}$, where δ_{Fi} is Kroenecker's delta. After ignition $f_F = 0$, and $f_i = \alpha_i$, i = O, P. The reaction term w_i is given by the Arrhenius expression:

$$w_i = \alpha_i B \rho_g^2 Y_F Y_o \exp(-E/\bar{R}T) \tag{16}$$

where E is the activation energy and $\bar{R}$ the gas constant. B is a frequency term and depends on temperature according to $B = B_o T^{\frac{1}{2}}$, where B_o is a constant. Using equation (14), equation (15) can be rewritten as follows:

$$\rho_g v \frac{dY_i}{dx} - \frac{d}{dx} \rho_g D_i \frac{dY_i}{dx} = w_i + \dot{m}(f_i - Y_i) \tag{17}$$

c. Energy conservation:

$$\rho_g v H_g - k \frac{dT}{dx} + \dot{H}_s = \text{constant} \tag{18}$$

where H_g is the gas enthalpy. H_g is given by the following equation:

$$H_g = \sum_i Y_i \int_{T_r}^{T} c_{pi} dT + H_i^o \tag{19}$$

where H_i^o is the standard enthalpy of formation for the gas at T_r and c_{pi} is the specific heat of species i. Using equation (19), equation (18) can be rewritten as follows:

$$\rho_g v H_g - \frac{k}{c_p}\frac{dH_g}{dx} + \dot{H}_s = \Psi \qquad (20)$$

where c_p is the gas specific heat. The constant Ψ in equation (20) is evaluated at the downstream boundary where the derivative with respect to x is assumed to be zero. The addition of heat to the mixture is accomplished by changing the value of this constant at the position of the heat source, by an amount equal to the added heat flux.

d. Equation of state:

$$\rho = pM/[(1-V_s)\bar{R}T] \qquad (21)$$

where V_s is the spray volume (equation 13) and M is the molecular weight of the mixture:

$$M = \sum_i 1/(Y_i/M_i) \qquad (22)$$

BOUNDARY CONDITIONS.

a. Upstream boundary conditions at $x = 0$ require a complete specification of the mixture in terms of temperature, speed, gas composition and droplet number density. For the present work the spray was polydisperse, the gas was air, and there was velocity equilibrium between the droplets and the gas. Equation (9) results in a non-zero droplet evaporation rate at the upstream boundary. Results were, therefore, obtained for a fixed distance between the upstream boundary and the plane heat source.

b. Downstream boundary conditions are expressed in terms of vanishing gradients for all variables involved. Thus, at $x = x_L$ it is required that $dY_i/dx = 0$ and $dH_g/dx = 0$, which implies the absence of liquid phase, or $N_j = 0$.

PROPERTY CALCULATIONS.

Properties were computed using the local gas temperature and mixture concentration. It is assumed that for dilute sprays the Lewis number ($\rho c_p D/k$) can be set equal to one. The properties under consideration are, therefore, k, D_i, μ and c_p. Following reference (19) for the molecular values of k

$$k = \sum_i n_i k_i \qquad (23)$$

and

$$\mu = \sum_k n_i \mu_i \qquad (24)$$

where n_i is the mole fraction of species i, while k_i and $_i$ are the molecular thermal conductivity and viscosity of the species. The specific heat is given by:

$$c_p = \sum_i Y_i c_{pi} \qquad (25)$$

Following reference (20) the individual species properties were expressed as linear functions of temperature.

For turbulent sprays the computed laminar transport coefficients k and D were augmented using the following relationships (13):

$$k_t = k + \rho c_p \varepsilon \tag{26}$$

and

$$D_{it} = D_i + \varepsilon \tag{27}$$

where k_t and D_{it} are the turbulent thermal conductivity and species diffusion coefficients, respectively, and ε is the eddy diffusivity. In turn:

$$\varepsilon = \lambda u' \tag{28}$$

where λ is a characteristic turbulent length scale of the approach flow and u' is the rms velocity fluctuation.

In the formulation described above, the burning velocity is not an eigenvalue. It is, instead, defined as the lowest upstream gas velocity for which the boundary conditions of the problem can be maintained. This is equivalent to calculating incipient "flashback" conditions for a liquid fuel spray streaming towards a hot source; for example, towards a region where burning of combustible material is already taking place.

NUMERICAL CALCULATION

Equations (3) and (4) and either (8) or (9) for a single droplet can be easily integrated using a step-by-step method beginning at the upstream boundary, provided that the gas profiles are known. In turn, equations (14), (17), and (20) and the boundary conditions for the gas, form a two point boundary value problem of first and second order non-linear ordinary differential equations, which require the spray coupling terms given by equations (11) through (13) for their integration. Following Williams' (6) suggestion, the following iterative scheme was used for the solution of the coupled set of spray and gas phase equations: beginning with assumed gas profiles, the equations for each droplet group were solved, and the coupling terms calculated. The coupling terms were then used in the solutions of the gas phase equations, thus providing profiles for new spray phase calculations, and so on. Convergence was achieved when there were negligible changes in the coupling terms between iterations:

$$S = \sum_m \left[\Delta(\dot{m}_m)^2 + \Delta(\dot{H}_{sm})^2 + \Delta(V_{sm})^2\right] \leq e \tag{29}$$

where the summation is taken over all grid points, m, Δ denotes differences between successive iterations, and e is a small positive number. The concentrations of species at the downstream boundary were checked for agreement with those calculated using the stoichiometry of fuel burning.

Regarding the details of the numerical integration, the first order differential equations for the spray (Equations 3, 4, and 8 or 9) were integrated beginning at x = 0 using Euler's predictor-corrector method. The gas phase species conservation equations are non-linear through the temperature and concentration dependent gas properties, but the main contribution

to non-linearity arises from the reaction term w_i in the species equations. Using the quasi-linearization method described by Fay et al (21), solution of equation (17) for i = F, O, and P was therefore approached through successive iterations involving a linearized form of w_i and its derivatives. The round-robin iteration scheme involved successive calculation of product, fuel, oxidizer and enthalpy profiles, in that order, using the results of each previous iteration for computing non-linear terms, until the non-linear species equation (16) was very nearly satisfied. The matrices involved in the integration of the gas phase equations are tri-diagonal and can be easily inverted. The matrix inversion process was started at $x = x_L$, and required a Raphson-Newton iteration scheme for matching with the upstream gas boundary conditions.

For a given spray, numerical solution of the equations could be obtained provided the upstream gas velocity was larger than the burning velocity. Decreasing the velocity eventually results in non-converging iterations with relatively large values of ^{e} (Eq. 29). Moreover, the temperature calculated during each iteration became progressively larger in the upstream direction. Therefore, the criterion for a non-converging solution was the calculation of a temperature exceeding the droplet ignition temperature at a convenient upstream point. The value of burning velocity was bracketed between adjacent gas velocity values corresponding to convergent and non-convergent solutions. With slight modifications the integration method was also used to compute the burning velocity in a premixed gas without a liquid phase. This was accomplished by setting the droplet number density equal to zero, and adjusting the upstream value of fuel mass fraction for the desired fuel concentration.

The calculations were carried out using the IBM 360-67 computer at Rutgers University. The CPU time depended on the fuel concentration and droplet radius, but averaged about three minutes for a convergent solution, and about five minutes to determine lack of convergence. For a given fuel concentration, decreasing the droplet radius results in a decrease in burning time of the spray. Consequently, sprays with very small droplets required a minute step size, Δx, and long computing times. For a monodisperse spray with an 8μm diameter droplets the CPU time for a convergent solution was approximately 20 minutes. Bracketing of the flame propagation velocities was accurate to ±5%.

Calculations were carried out for monodisperse tetralin-air sprays (4), and polydisperse kerosene-air sprays. Thermodynamic properties of liquid tetralin were obtained from the Handbook of Chemistry and Physics (22). Table I lists pertinent physicochemical properties of kerosene that were used in the calculations. The properties of fuel vapor were assumed to be those of decane and were obtained from correlations used by Faeth et al (20).

The heat source intensity was sufficient to increase the pure air stream temperature by approximately 1200°K. The computed burning velocities were insensitive to the choice of heat source intensity, provided the resulting temperature was sufficiently high for consumption of fuel vapor.

TABLE 1. PROPERTIES OF KEROSENE

Density:	0.8 gm/cm^3
Heat Capacity:	0.64 cal/gm^oK
Latent Heat of Vaporization:	61 cal/gm
Heat of Formation (liquid):	598 cal/gm
Heat of Reaction:	10,400 cal/gm
Chemical Formula:	$C_{12}H_{26}$
Stoichiometric Coefficient for Oxygen:	3.48
Stoichiometric Coefficient for Products:	4.48
Physical Properties of the Vapor and the Products of Combustion:	Decane Vapor (20)
Boiling Point:	483^oK

For the calculations reported in this work $v_o = u_{jo}$ and $T_o = T_{jo}$ except as noted. The step size was between 0.5×10^{-3} and 5×10^{-3}cm, and the integration region extended 0.2 to 0.5 cm upstream from the heat source, and 0.2 cm to 0.5 cm in the downstream direction depending on the droplet size.

RESULTS AND DISCUSSION.

RESULTS OBTAINED USING A PRESCRIBED GAS TEMPERATURE AS THE IGNITION CRITERION OF THE LIQUID DROPLETS. A discussion of calculated burning velocities of laminar tetralin-air sprays is found in reference 4. These were obtained using various prescribed gas temperatures as the conditions for ignition of the liquid droplets and as a result the ignition delay of the droplets is underestimated. The present report contains additional results obtained using the ignition criterion described by equation (1). The new results are qualitatively similar to those of reference 4, but more realistic since the ignition delay period of the droplets is taken into account.

CHOICE OF THE PARAMETERS B_o AND E FOR FUEL VAPOR-AIR MIXTURES. Published experimental data on premixed flame burning velocities was used for obtaining appropriate values of the pre-exponential factor, B_o, and the activation energy, E, which are necessary for describing the homogeneous gas phase reactions in the spray model. This was accomplished by matching available experimental laminar burning velocities with calculated results using assumed pairs of B_o and E. Reference 23 gives a value of 40 cm/sec for the maximum laminar burning velocity of a kerosene vapor-air mixture at an equivalence ratio* of 1.06. Figure 2 shows computed burning velocities which were obtained using $B_o = 4 \times 10^{12} sec^{-1}$ and E = 40,000K cal/gmole The experimental point at 40 cm/sec (23) is in good agreement with the calculated results. Similar results were obtained for tetralin-air vapor mixtures, and resulted in $B_o = 5 \times 10^{12} cm^{-1}$, and E = 40,000 cal/gmole. The present value of B_o is different than that employed in reference 4 because the experimental data that was used for the matching process in the previous work was actually spray data with 8μm diameter droplets, which did not accurately represent the fuel vapor behavior.

MONODISPERSE TETRALIN-AIR SPRAYS. Figure 3 shows the effect of fuel concentration on the calculated laminar burning velocity of monodisperse tetralin-air sprays with 15 m diameter droplets. On the same Figure are included calculated results from reference 4 for various values of the prescribed gas temperature for droplet ignition, T_I, for comparison with the present results which were obtained using equation (1) as the ignition criterion for the liquid droplets. Both methods of describing the conditions of droplet ignition yield a qualitatively similar dependence of burning velocity on fuel concentration. However, the use of equation (1) seems

*The equivalence ratio is defined as the ratio of the actual over the stoichiometric fuel-air ratio.

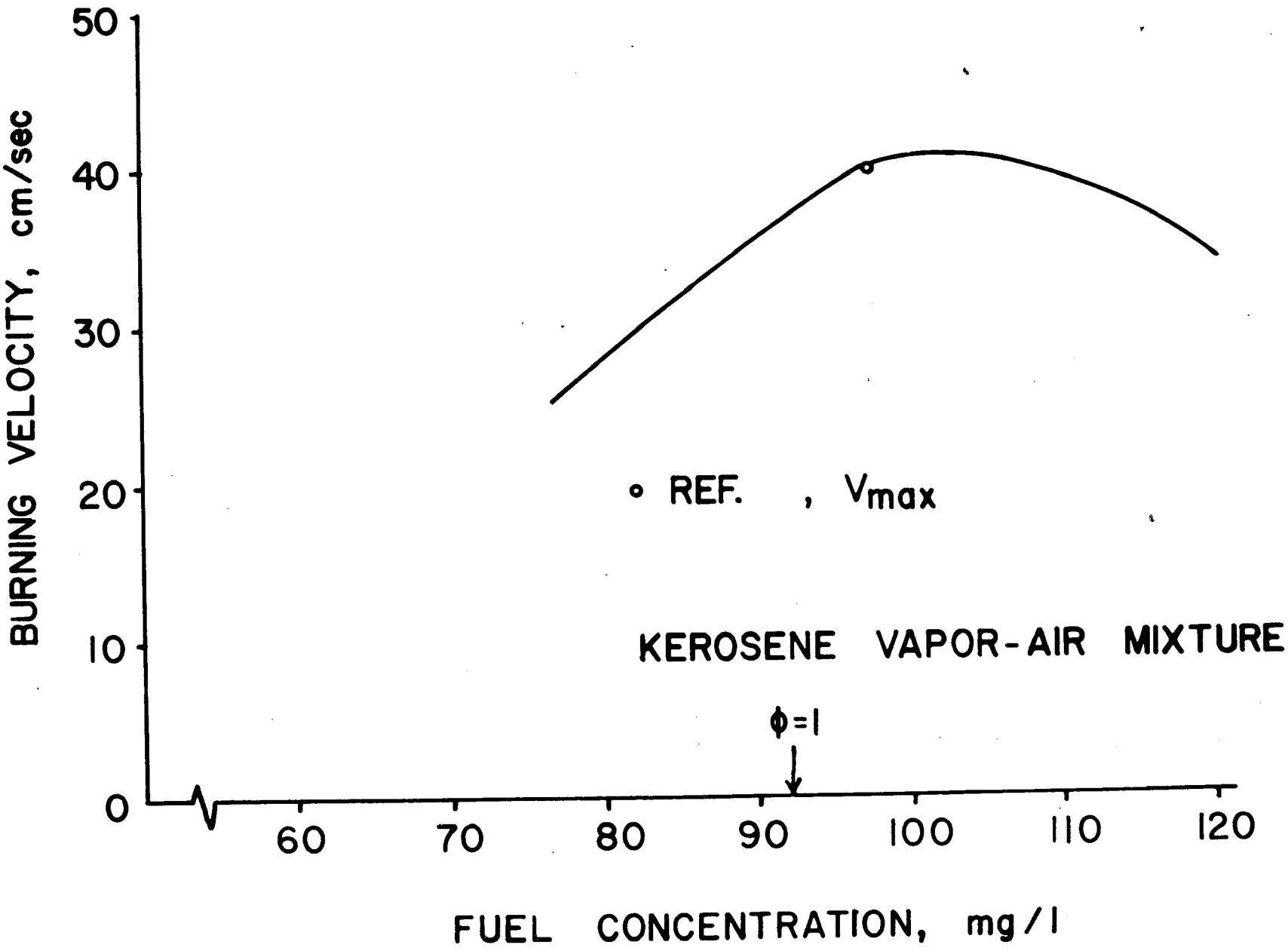

FIGURE 2. BURNING VELOCITIES OF KEROSENE VAPOR-AIR MIXTURES

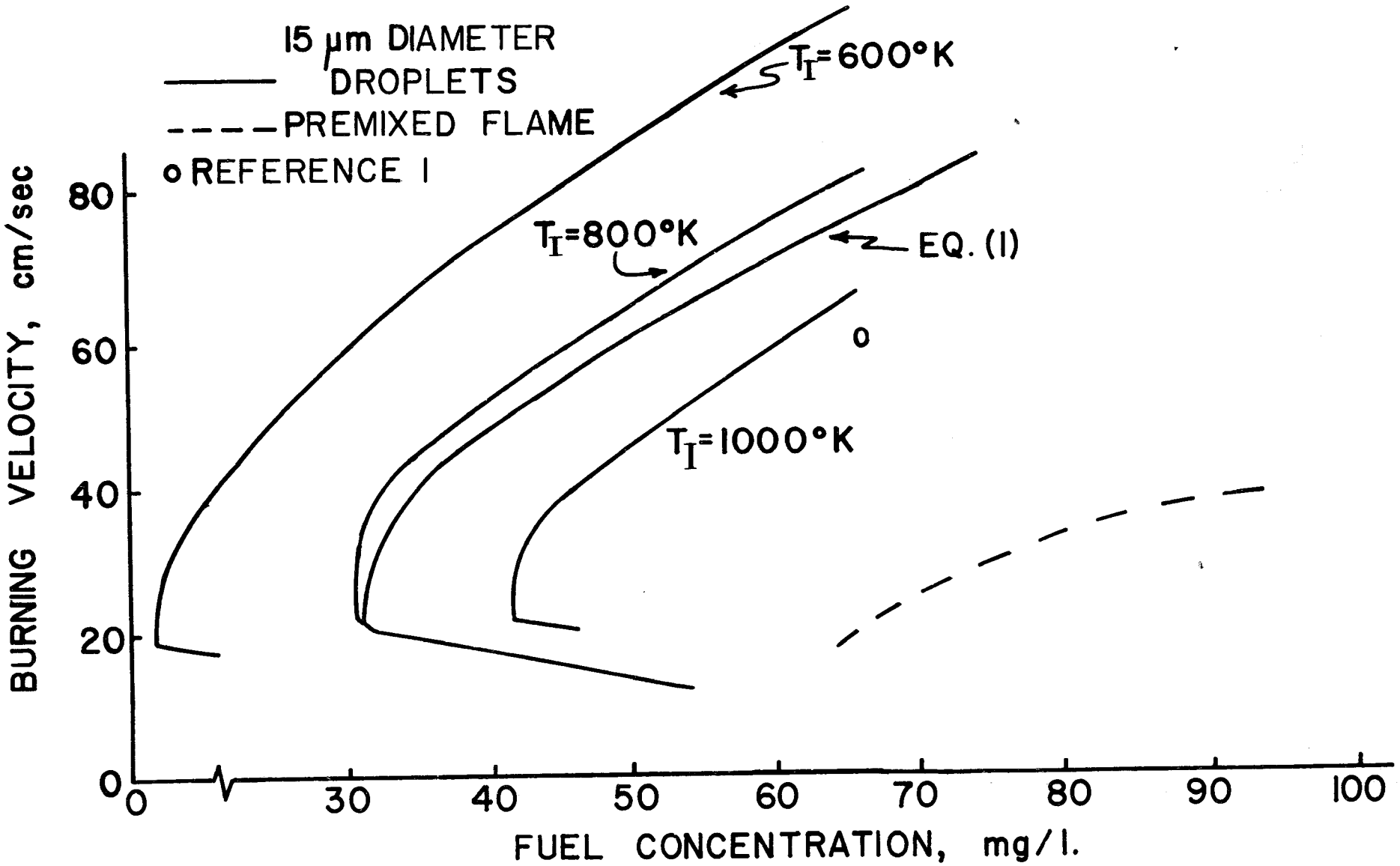

FIGURE 3. BURNING VELOCITY VS. FUEL CONCENTRATION FOR MONODISPERSE TETRALIN-AIR SPRAYS. DROPLET DIAMETER IS 15μm

to be more convenient because it does not require the use of T_1 as an input to the calculations. In addition, it results in a burning velocity of 76 cm/sec at a fuel concentration of 69 mg/l which is in reasonable agreement with the experimental point of reference 1, also shown on Figure 3.

Calculated burning velocities for a premixed gas are also shown on the same figure, and are lower than those in the mist with equivalent fuel concentration. For relatively low fuel concentrations Figure 3 shows that it is possible to have two different speeds of flame propagation in a spray. The higher upper branch of the curve is associated with heterogeneous combustion around the droplets with very little preignition vaporization. The lower branch of the curve describes the mist as it moves very slowly towards the flame, and there is appreciable time for preignition vaporization. Since the pure vapor has a lower burning velocity than the 15μm mist, the effect of preignition vaporization is a double valued burning velocity at the same fuel concentration. Similar behavior can be shown for large droplets. However, as the droplet size increases at fixed fuel concentration, appreciable preignition vaporization in a spray occurs for speeds which are too low to be of practical significance.

Figure 4 shows the effect of droplet diameter on the laminar burning velocity of tetralin-air sprays of fixed fuel concentration at 69 mg/l. Beginning with sprays of large droplets, decreasing the diameter results in increasing the burning velocity, since the burning rate of a monodisperse fuel spray with constant initial fuel concentration is inversely proportional to the square of the droplet radius. Eventually, as the droplet diameter becomes very small the droplets completely evaporate before reaching the ignition temperature of the liquid fuel, and the burning velocity approaches that of a premixed gas. For small droplets the final decrease in burning velocity as the droplet diameter decreases is, therefore, due to the transition from a heterogeneous to a premixed gas burning mechanism. Thus the curve on Figure 4 has a maximum at a droplet diameter between 0 to 15μm. At zero diameter the burning velocity is that of a premixed gas.

It should be noted that the calculated burning velocity at 8μm droplet diameter, which is shown on Figure 4, corresponds to flame propagation with appreciable liquid preignition vaporization or to the lower branch of a curve similar to that shown on Figure 3 for 15μm diameter droplets. The second higher burning velocity solution, which corresponds to the upper branch of the curve, results in a burning velocity of 120 cm/sec. The use of the lower branch solution is justified because of agreement with previous experimental data as will be shown in the next section. Rigorous justification for this choice will have to await further study.

The following section presents experimental data which confirm the influence of droplet diameter on burning velocity which is predicted by results such as those shown on Figure 4. A qualitative discussion of possible mechanisms for flame propagation in a spray will also be discussed in that section.

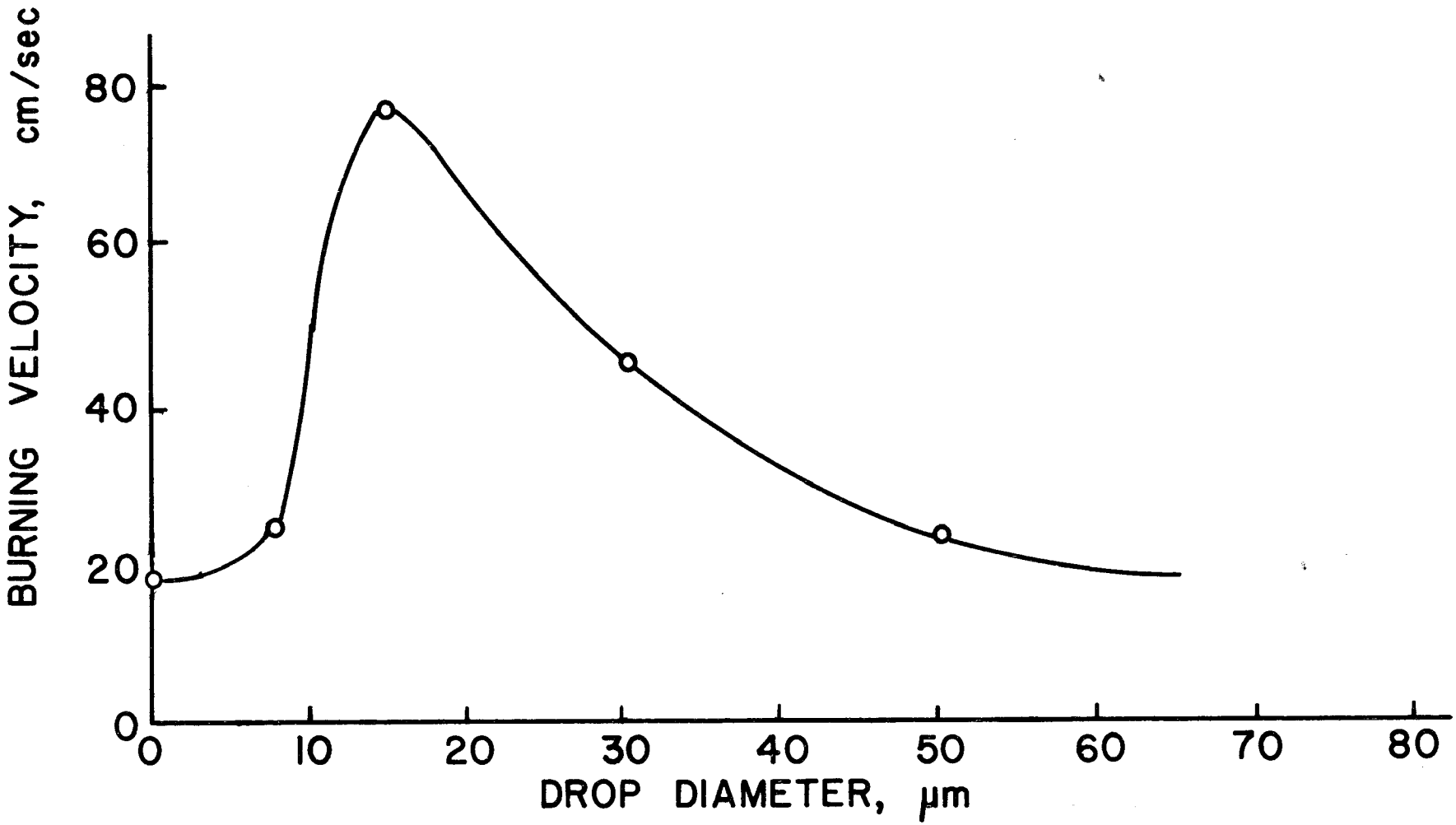

FIGURE 4. DROP DIAMETER VS. BURNING VELOCITY FOR MONODISPERSE TETRALIN-AIR SPRAYS. FUEL CONCENTRATION IS 69 mg/l

COMPARISON OF CALCULATED BURNING VELOCITIES WITH AVAILABLE EXPERIMENTAL DATA. Table 2 can be used for comparing burning velocities with presently available experimental data. The experimental measurements are those of Burgoyne and Cohen (1) for monodisperse tetralin sprays, as well as one point obtained during the present work using turbulent polydisperse kerosene-air sprays. For the turbulent flow calculations the upstream turbulent intensity was 8%, and the turbulence scale was 0.3 cm. There were equal to the experimentally measured turbulence intensity and the O.D. of the pilot flame tube, respectively. Agreement between predicted and measured values for tetralin is satisfactory except for the relatively large droplet diameter of reference 1. It should be noted that for droplets larger than approximately 20μm, the experimental procedure of reference 1 consisted in measuring the mean burning velocity using direct photographs of highly asymmetric flames anchored at the mouth of a tube. For droplets smaller than 20μm, the flame had a well-defined flame cone, and could be photographed using a shadowgraph method.

EXPERIMENTAL WORK

PREVIOUS WORK ON THE EFFECT OF DROPLET SIZE ON THE BURNING VELOCITY OF LIQUID-AIR SPRAYS.

The effect of droplet size on the burning velocity of liquid fuel sprays has been studied by several investigators to date. The experiments of Burgoyne and Cohen (1) using monodisperse tetralin-air sprays showed that the laminar burning velocity in sprays with very small droplets is smaller than the burning velocity in comparable sprays of larger droplets. Moreover, very small droplets appear to vaporize completely upstream of the flame front, thus giving the flame a premixed gas flame appearance, while large drops burn in diffusion flames around the liquid phase, thus giving the flame a "brush" type appearance. Unfortunately, the air-fuel ratio in Burgoyne and Cohen's experiments was not constant over a wide range of droplet diameters for finding a critical diameter for maximum burning velocity at constant air-fuel ratio.

The following mechanism for flame propagation can be used to qualitatively interpret the experimental results: In sprays of large droplets the flame propagation is in relatively vapor-free space with a relay process across the diffusion flames surrounding each droplet. Heterogeneous combustion around the droplets takes place in the optimum air-fuel ratio, and the droplets act as high temperature heat sources for the ignition of adjacent droplets, thus resulting in flame propagation with pockets of cool air remaining between the droplets. In addition, the thermal expansion of the gas around the burning droplets intensifies the transport process, and accelerates the burning velocity. At constant air-fuel ratio, beginning with relatively large droplets, an initial reduction in a droplet size results in a more closely spaced suspension, a higher volumetric heat release rate, and consequently an increase in burning velocity. However, further decrease in droplet size eventually results in significant amounts of fuel evaporating ahead of the flame and mixing with the air between the droplets.

TABLE 2. CALCULATED VS. EXPERIMENTAL BURNING VELOCITIES

Flow	Fuel	Drop Diameter (μm)	Mass Concentration (mg/l)	Burning Velocity Experimental (cm/sec)	Burning Velocity Calculated (cm/sec)
laminar	Tetralin	15	69	59	76
laminar	Tetralin	22	64	55	42
laminar	Tetralin	30	60	67	35
laminar	Tetralin	38	48	58	23
Turbulent	Kerosene	Polydisperse Spray A	69	60	67

Burning of this lean homogeneous fuel-air mixture requires high temperatures, or a relatively large amount of heat transferred ahead of the flame for ignition. As a result, for the relay flame transfer associated with heterogeneous combustion around the droplets, an increase in the amount of fuel evaporated before ignition will also decelerate the burning velocity. Thus, increasing the droplet size in such a spray may result in increasing the burning velocity. Although this was not confirmed by previous experimental investigations, an interesting conclusion of the previous results is that there is a range of droplet diameters for maximum burning velocity in a spray, and that very find atomization may not always be desirable in combustion applications.

A quantitative interpretation of the transition from heterogeneous to homogeneous combustion in a spray, and of the accompanying influence on burning velocity, must take into account the relative magnitudes of the characteristic ignition delay and burning times for individual droplets and for a premixed gas. According to Williams' (6) approximate analysis, it is expected to have both increases and decreases in burning velocity upon transition from heterogeneous to homogeneous combustion in a spray depending on the properties of different fuel oxidizer systems. Reference 4, using several different ignition delay times for the droplets, shows how this transition process can result in a maximum value for the calculated burning velocity as the droplet diameter decreases at constant air-fuel ratio. References 24 and 25 include discussions of a possible decrease in air-fuel ratio as the spray particle size decreases in the lean limit for flame propagation.

Mizutani and Nakajima(10) used an open inverted-cone-flame burner, and measured the local rate of flame spread in turbulent kerosene-mist-propane-air mixtures. The normal rate of flame spread, S_u, into the mixture was defined in terms of the expression $S_u = \overline{V} \sin \overline{\theta}$, where $\overline{V}$ is the local mean flow speed and $\overline{\theta}$ is the angle between the mean position of the flame front and of tracks from every small droplet in the flow. Since droplets track the flow streamlines according to their size, it is not clear why it is appropriate to use tracks from small droplets for the measurement of $\overline{\theta}$ in polydisperse sprays.

The measurements in reference (10) were carried out in a region of relatively constant average gas speed and turbulence intensity. It is, therefore, assumed that flame elements reach their "equilibrium" speed of propagation in that region so that the measured value of S_u is the burning velocity of the mixture. Data in reference (10) shows that for the same upstream conditions and overall air-fuel ratio, addition of kerosene spray to a propane-air flame increases the burning velocity while addition of kerosene mist consisting of very fine droplets may produce the opposite effect. It was concluded that the measured changes in burning velocity, as the kerosene is added in relatively large droplet or mist form, are a consequence of the presence of the mist, and not of the different physicochemical properties of kerosene and propane vapor. Thus, this conclusion is also in support of the previous qualitative description of the effect of droplet size on the burning velocity.

The present work is an experimental investigation of the effect of droplet size on the burning velocity of polydisperse kerosene-air sprays. The experiments were similar to those in reference (10), and the normal rate of flame spread into the combustible mixture, measured in a region of relatively constant mean flow speed and turbulent intensity, will be identified as the burning velocity of the mixture for the turbulence level present in the apparatus. No rigorous justification for this assumption is attempted here. However, from schlieren photographs it appears that the flame front is flat in that region, suggesting a constant speed of flame propagation.

EXPERIMENTAL APPARATUS AND PROCEDURE.

The experimental apparatus was similar to that used in reference (10) and is shown schematically on Figure 5. It consisted of a vertical stainless steel tube 24 mm I.D. and 1 m long with kerosene-air spray flowing upwards and discharging into the ambient atmosphere. A small acetylene pilot flame, with a 3 mm O.D. burner, was located at the exit of the tube and was used to ignite the spray. The resulting inverted cone flame was photographed using a schlieren system. The primary air supply was metered using a rotometer, and a second rotometer was used for measuring the air supply to an ultrasonic atomizing nozzle operating at 35,000 cps which was employed for atomizing the liquid fuel. The fuel was supplied to the nozzle through a variable flow rate rotary pump, and the air-fuel ratio, as well as the droplet size distribution, were set by adjusting the pump exit pressure, and the primary and atomizing air flow rates. The air-fuel ratio was calculated from the rotometer readings, and by weighing the mixture collected at the tube exit using a plastic bag. The kerosene and air flow rates were constant for all the experimental runs, and the air-fuel ratio was 18.

Figure 6 shows the distribution along the tube radius of mean velocity and rms velocity fluctuations upstream from the flame front at the tube exit measured using hot wire anemometry. The flow Reynolds number based on the tube diameter was 2700. The rms fluctuations shown are average values including turbulent bursts due to the transitional flow regime.

Droplet diameters were measured from photographs of the spray obtained using an instantaneous light source with a flash duration of approximately 5μ sec. The optical system was similar to that used by Ingebo (26), and produced a magnification of X8 on the film with a depth of field of approximately 1 mm. To avoid excessive attenuation of the light passing through the fine spray, a 10 mm wide slit was placed perpendicular to the light beam over the tube exit when photographing the droplets. Photographs were taken only at one position corresponding to a distance of half a tube radius from the tube centerline and from the tube exit. Droplet sizes were measured after magnifying the negatives about 3 times. About 300-650 droplets were counted using several negatives for each run. The droplet sizes measured with this method are subject to uncertainty because of (a) personal interpretation of the position of the droplet boundaries, as well as of the droplets which are out of focus, and (b) the effect of film developing time on the image size of the very small droplets. The counting and film developing were carried out by the same person to minimize differences in interpretation and developing technique. The resulting droplet size counts were used to qualitatively describe the relative extent of atomization between different sprays. This was accomplished by comparing the liquid volume in

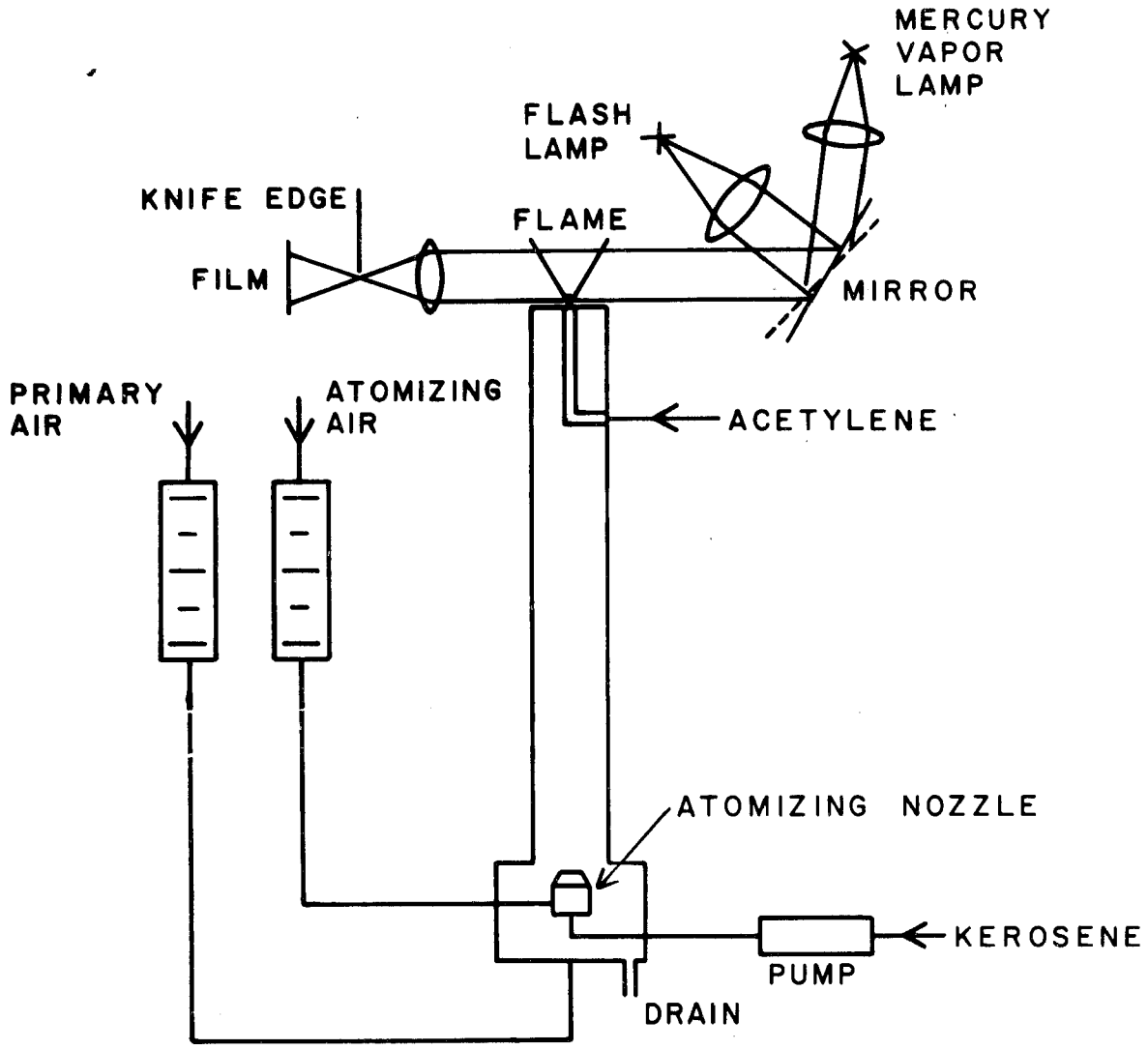

FIGURE 5. SCHEMATIC DIAGRAM OF THE EXPERIMENTAL APPARATUS

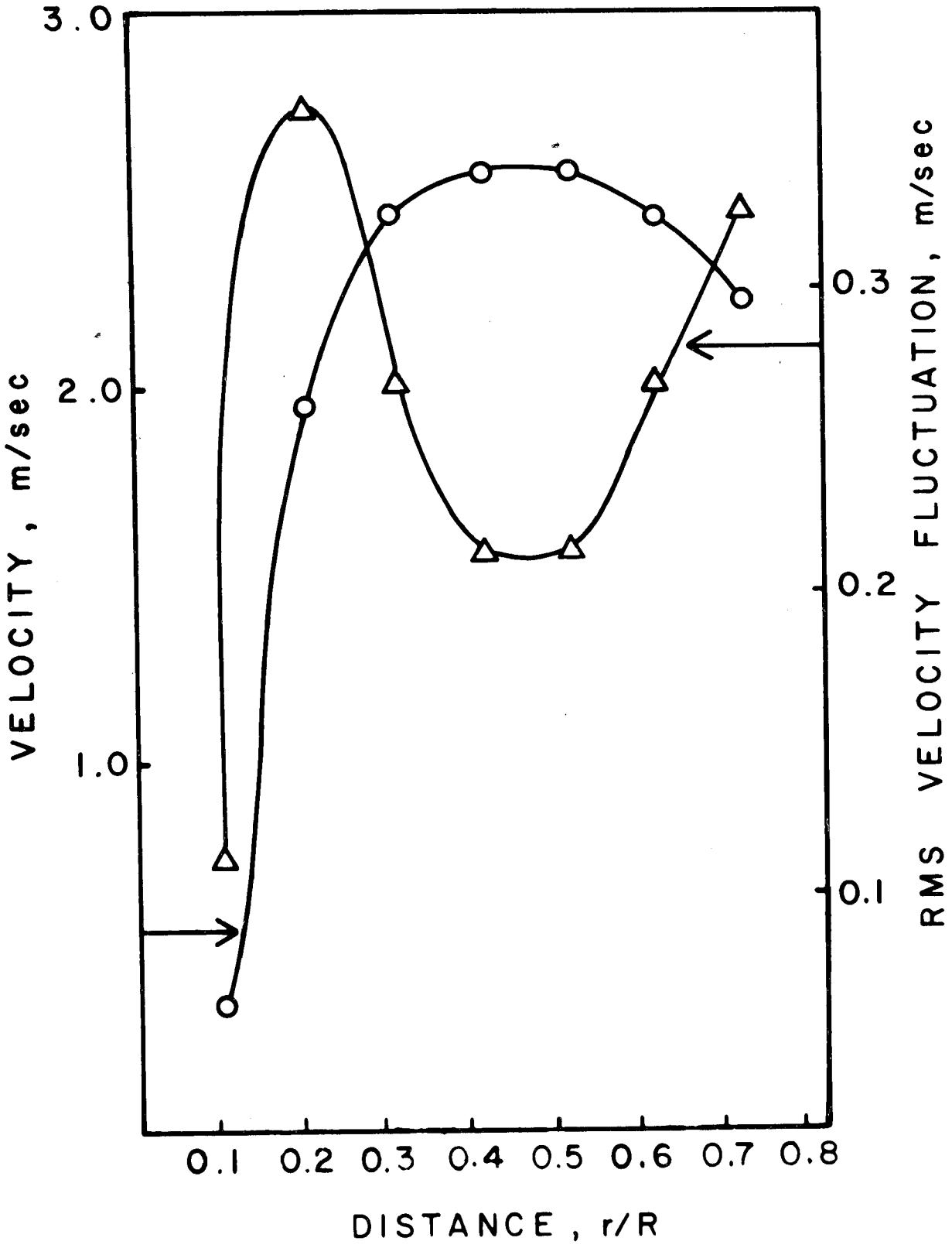

FIGURE 6. MEAN AIR VELOCITY AND RMS VELOCITY FLUCTUATIONS AT THE TUBE EXIT

each droplet size group for the sprays tested. Droplets that appeared smaller than 30μm in diameter were not included in the results because their diameters could not be measured accurately with the present system.

Figure 7 shows schlieren images of flames obtained for three different degrees of atomization. The exposure time was 1000^{-1} sec, the magnification was X3 on the film, and the depth of focus was about 6 mm. The light source was a high pressure mercury vapor lamp. Droplet streaklines can be clearly observed ahead of the flame using the photographic negatives, and can be used to track the mean position of particle paths in the flow. Occasional large scale turbulent bursts produced large scale distortions of the flame front, and only photographs where the flame front appeared smooth were used for measurements.

The burning velocity, S_u, was calculated using the relation $S_u = \overline{V} \frac{r_1}{r_2} \frac{\Delta r}{\Delta \ell}$ which is derived from the diagram on Figure 8. $\overline{V}$ is the mean flow velocity over a length Δr, measured at the tube exit and at a radial distance of half the tube radius, and $\Delta \ell$ is defined in terms of the surface enclosed by the mean particle path lines from Δr to the flame front. r_2 is the mean distance of $\Delta \ell$ from the tube centerline. It should be noted that $\Delta \ell$ appears as a straight line in the region of measurement. This method of calculating S_u minimizes the error due the differences in the mean position of streamlines and droplet path lines, since differences at large and small radii tend to cancel out. As it turned out this method of calculating S_u yielded values approximately 10% lower than those obtained by the angle method of reference (10).

RESULTS AND DISCUSSION

DEGREE OF ATOMIZATION IN THE SPRAYS TESTED. Figure 9 presents direct photographs of spray flames showing the effect of increasing fuel atomization on flame appearance. Figure 9a is for spray A consisting of relatively large droplets which burn enveloped in yellow diffusion flames. Combustion appears to take place downstream of a well-defined region that does not necessarily coincide with the flame front recorded on schlieren photographs. Increasing atomization in sprays C and E (Figures 9b and 9c) results in decreasing the number of individually burning drops, and in the gradual appearance of a blue flame front which is characteristic of premixed gas flames. Spray E is for the finest atomization that was used in the present tests and shows a well-defined blue flame front with a small number of burning drops in the downstream region.

Figure 10 shows the cumulative volume distribution versus droplet diameter for sprays A to E calculated from the droplet size counts. The liquid and air-flow rates were the same for all tests. As a result, the liquid volume in each size range was normalized with respect to the total volume of spray A. Spray A consisted of relatively large drops whose diameter could easily be measured. Figure 10 gives no information about the important droplet diameter range below 30μm. However, it shows that from spray A to spray E, (a) the number of large diameter droplets decreases, and (b) the fluid volume atomized in droplet diameters below 30μm increases. Thus, the results on Figure 10, together with the direct photographic observations of the spray flame, confirm that from spray A to spray E the atomization becomes progressively finer.

(a) SPRAY A

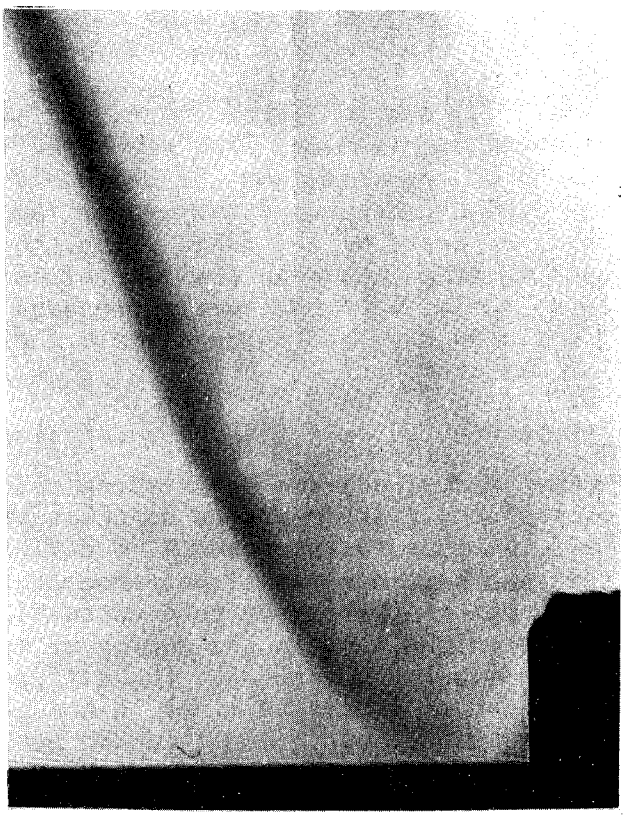

(b) SPRAY C

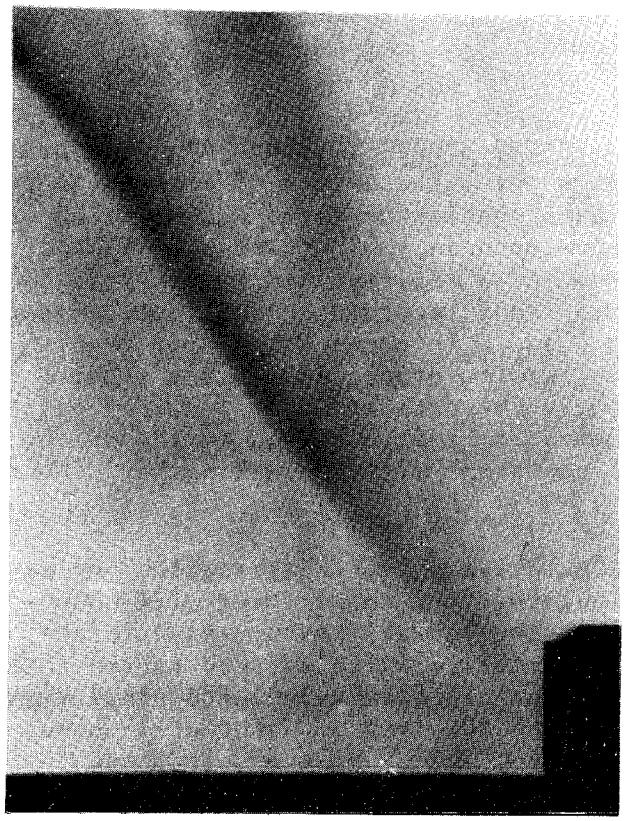

(c) SPRAY E

FIGURE 7. SCHLIEREN IMAGES OF FLAME FRONT

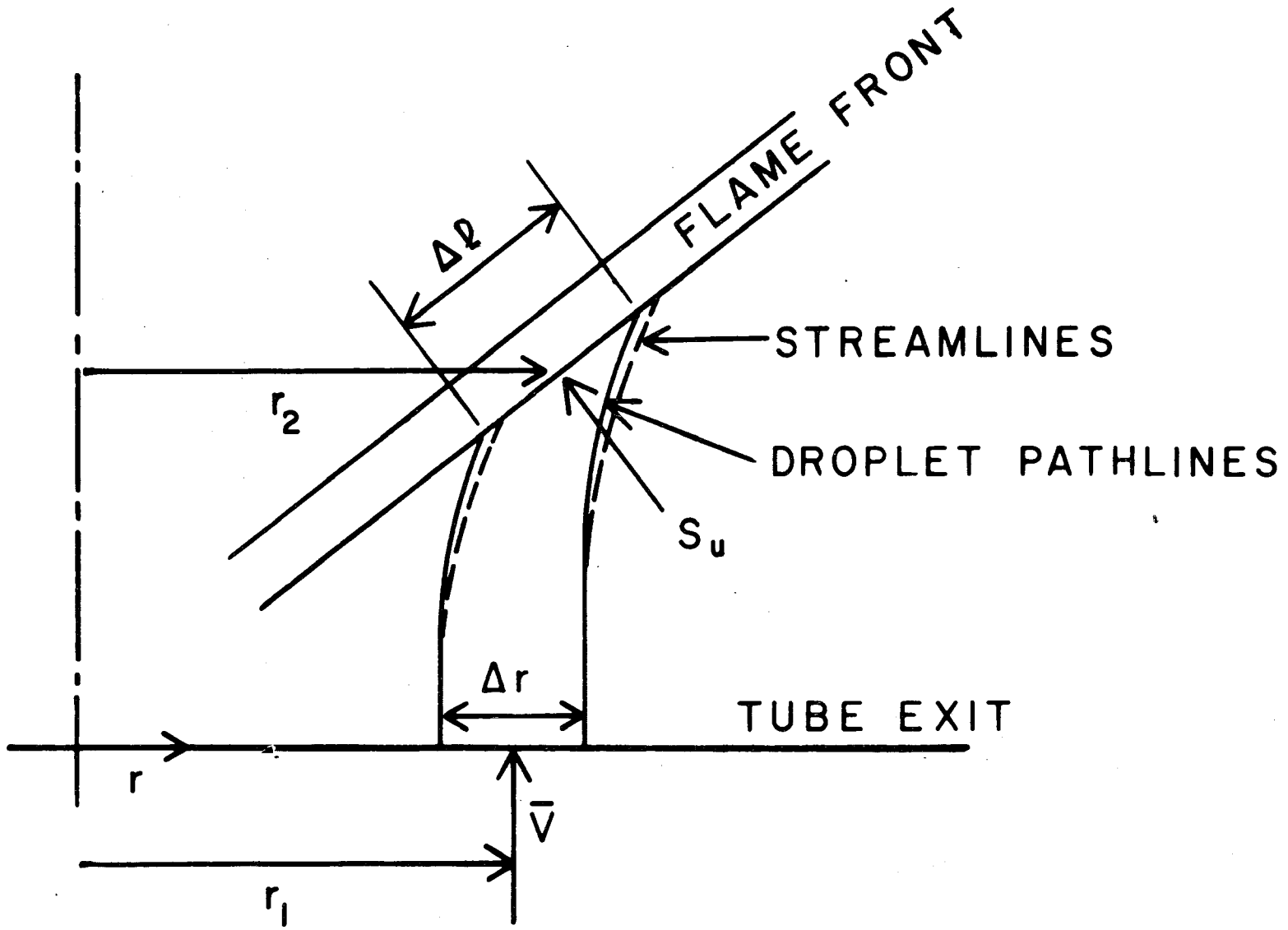

FIGURE 8. SCHEMATIC DIAGRAN USED FOR CALCULATING S_u

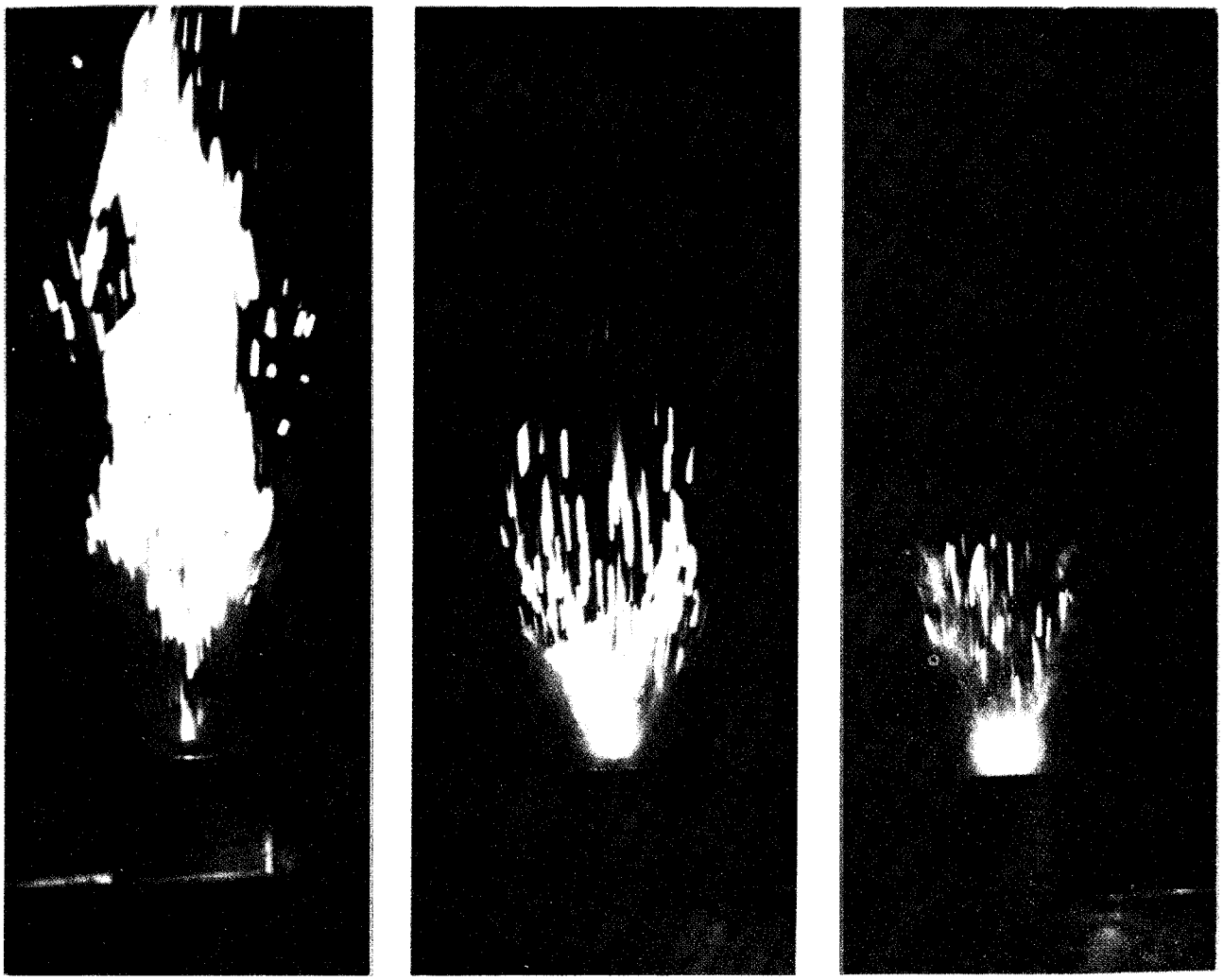

(a) SPRAY A (b) SPRAY C (c) SPRAY E

FIGURE 9. DIRECT PHOTOGRAPHS OF SPRAY FLAMES

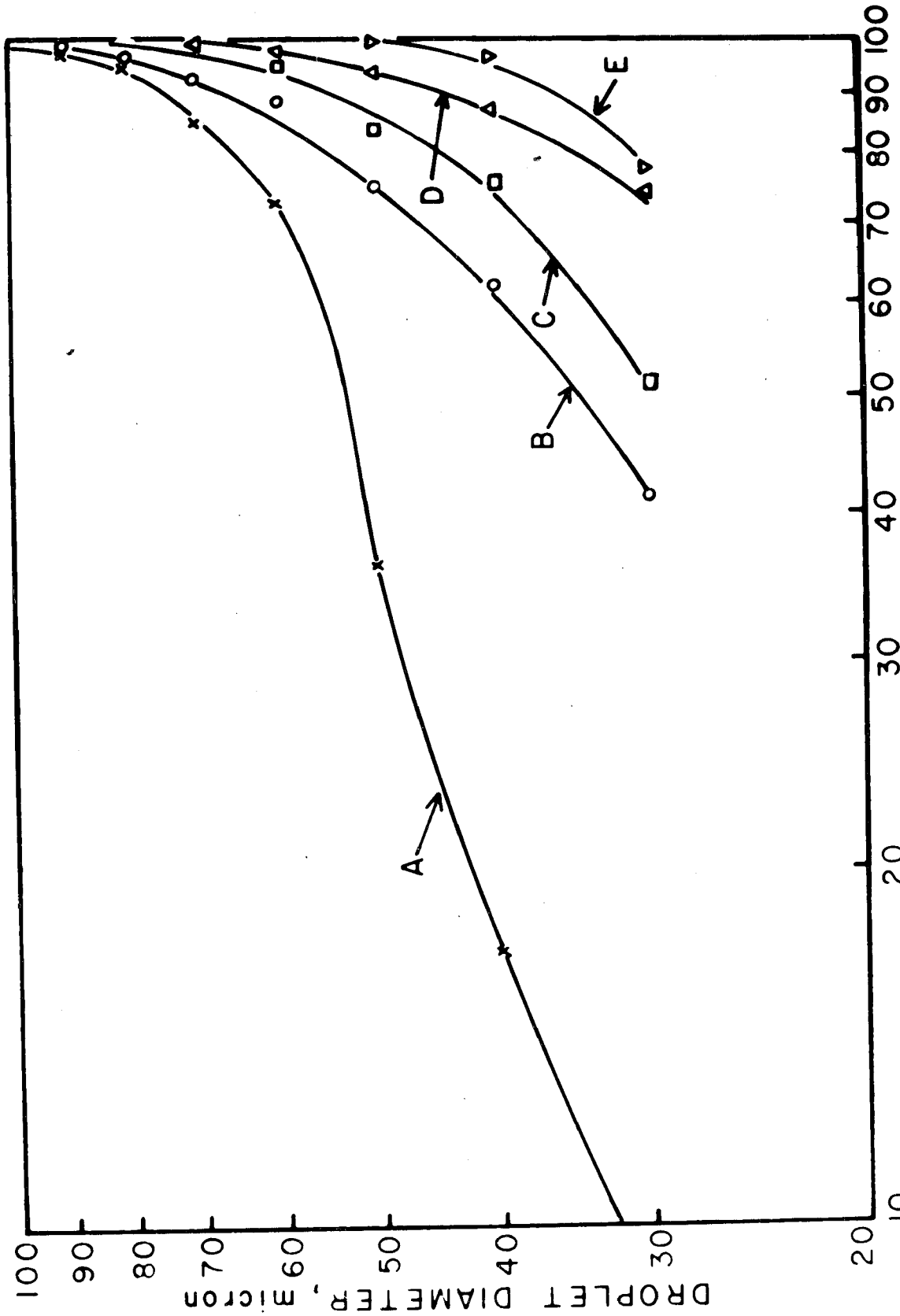

FIGURE 10. CUMULATIVE NORMALIZED VOLUME FOR THE SPRAYS TESTED

From the data it is possible to estimate the number density of the droplets in spray A, assuming a uniform spatial particle distribution. Table 3 shows the droplets counted per cm^2 of focal plane measured from photographic negatives, together with the calculated number density (droplets/cm^3) for each size group. The combined number density for spray A is thus estimated at 1750 droplets/cm^3. Using Table 3 and the liquid fuel density (0.8 gm/cm^3) it is possible to estimate the liquid concentrations at 6.8×10^{-5} gm/cm^3. This compares favorably with the value of 7.1×10^{-5} gm/cm^3 which is measured directly at the tube exit, and suggests that for spray A the measured particle size distribution includes practically all the droplets in that spray. Our inability to measure diameters below 30μm prevents us from making similar calculations for the other sprays tested.

BURNING VELOCITY RESULTS. Table 4 shows the burning velocities (S_u) measured for the sprays tested. The velocities are average values from several different measurements. It was estimated that measurements from photographic negatives resulted in a ± 4 cm/sec error in the calculated values of S_u. Reproducibility between different measurements was within ± 5 cm/sec from the average values of S_u shown on Table 4. S_u initially increased from 60 cm/sec for a relatively coarse spray to a maximum of 91 cm/sec as the degree of atomization increased. However, further atomization resulted in a decrease in burning velocity to 50 cm/sec for spray E, which for the present tests appeared to burn mostly as a premixed flame. It should be noted that the laminar burning velocity of kerosene vapor is reported as 40 cm/sec at an air-fuel ratio of 14 (23). From the results of Table 4 it appears that for a given kerosene-air mixture, there is a drop size distribution which results in a maximum rate of flame propagation, which is larger than that of a premixed gas of the same air-fuel ratio.

Observation of schlieren images of the flame front such as those on Figure 7 shows that as expected, the flame appears to be ignited in the boundary layer ahead of the pilot tube tip, and that the point of ignition is further upstream for spray C which had the maximum measured burning velocity. In addition, it should be noted that the angle of the flame with the vertical axis is not a true indication of burning velocity, because the effect of flow angle at the flame front must also be considered. Observation of the sample photographs on Figure 7 shows that the particle tracks appear to diverge outwards at the flame front by an increasing amount as the degree of atomization increases. This is because the zone of fuel burning (in gaseous or droplet form) downstream from the flame front is shortened as the droplet size decreases, thus increasing the effect of flame thrust, which is the reason for the diverging droplet pathlines at the flame front.

Reference 9 gives the following empirical correlation for the burning velocity of kerosene-air sprays in apparatus similar to that used in the present study:

$$S_u = \frac{6.800}{\bar{d}}(\phi - 0.012)\ (u')^{1.15}\ [\text{m/sec}] \qquad (30)$$

where ϕ is the fuel-air ratio, $\bar{d}$ is the Sauter mean diameter in microns, and u' is the rms velocity fluctuations in m/sec. For spray A and the

TABLE 3. DROPLET NUMBER DENSITIES FOR SPRAY A

Diameter Range, μm	Droplets/cm^2 (counted)	Droplets/cm^3
31 - 40	91	868
41 - 50	51	364
51 - 60	59	453
61 - 70	12	41
71 - 80	6	15
81 - 90	1	1
91 - 100	1	1
		1742

TABLE 4. BURNING VELOCITIES (AIR-FUEL RATIO = 18) KEROSENE-AIR SPRAYS

Spray	$\overline{V}$ cm/sec	u' cm/sec	S_u cm/sec
A	266	22	60
B	↓	↓	72
C			91
D			60
E			50

value of $\bar{d}$ can be calculated and is 54μm. For $\phi = 0.055$ and $u' = 22$ cm/sec, the value of S_u is calculated as 94 cm/sec, and should be compared with the measured value of 60 cm/sec for spray A. The poor agreement is probably due to the poor accuracy of the empirical correlation which was obtained in reference (10) using data with considerable scatter.

CONCLUSIONS

A mathematical model was developed which is capable of predicting the burning velocity in polydisperse air-fuel sprays given the initial conditions of the liquid and gas phases. The analytical predictions were tested against previous experimental data using monodisperse tetralin-air sprays, and the agreement was satisfactory.

The burning velocity in open polydisperse kerosene-air sprays was measured at constant air-fuel ratio and for various degrees of atomization of the spray. The results showed that as the degree of atomization increases, the burning velocity first increases to a maximum value, and then decreases to a burning velocity approaching that of a premixed gas mixture. This result is also predicted by the mathematical model. For one of the sprays tested, it was possible to accurately measure the upstream droplet size distribution. For that spray comparison between measured and calculated burning velocities was satisfactory.

In view of the good agreement between the analytical and experimental predictions, it is concluded that the mathematical model can be used with sprays produced during wind tunnel or field testing of aviation fuels. Calculations using modified fuel sprays produced by wind shear in a wind tunnel will be carried out in the near future when the spray data from the 5 ft wind tunnel at NAFEC becomes available.

Further work is currently being carried out in order to assess experimentally the effect of upstream air and fuel temperature on burning velocity. In addition, a holographic method for particle size measurement is currently being developed. These will provide additional data for checking the theoretical model. Regarding the use of the holographic technique it is expected that it will find useful application during wind tunnel and field spray tests of modified and heat fuels.